Available online at www.sciencedirect.com
SCIENCE DIRECT
Spectrochimica Acta Part A 63 (2006) 987–993
SPECTROCHIMICA ACTA PART A
www.elsevier.com/locate/saa

Spectral measurement of the caesium D_2 line with a tunable heterodyne interferometer

Luca Spani Molella, Rolf-Hermann Rinkleff*, Karsten Danzmann

Max-Planck-Institut für Gravitationsphysik, Albert-Einstein-Institut, Hannover and Institut für Atom- und Molekülphysik, Universität Hannover, Callinstraße 38, D-30167 Hannover, Germany

Received 6 September 2005; received in revised form 21 October 2005; accepted 31 October 2005

Abstract

The optical properties of a caesium atomic beam driven on a resonant hyperfine transition in the D_2 line were studied as a function of the probe laser frequency. Using a third off-resonant laser system, a heterodyne interferometer allowed simultaneous absorption and phase shift measurements of either the probe or the coupling laser. The signal features of the probe and coupling laser transmitted intensities showed strong differences in the vicinity of the hyperfine transitions excited by the probe laser. Regular absorption signals and electromagnetically induced transparency were found in either transmitted intensities. Furthermore, light induced birefringence of the probe laser was measured.

PACS: 39.30.+w; 42.50.Gy; 78.20.Fm

Keywords: Heterodyne interferometer; Tunable diode laser; Electromagnetically induced transparency; Light induced birefringence

1. Introduction

Absorption and emission of monochromatic light in two-level atomic transitions are well understood processes in quantum optics [1]. Their properties can drastically change if transitions to a third or a fourth level are included. In three-level atomic systems interacting with two coherent laser fields, coherent population trapping occurs if, for instance, two ground hyperfine levels couple to a common excited level. In this case the atoms are prepared in a non-absorbing state [2] and this effect is commonly known as electromagnetically induced transparency. In contrast to a dark coherence, an absorption enhancement can be observed in degenerate two-level atomic systems at the line centre, when the two laser fields have equal frequencies (electromagnetically induced absorption [3]). Combined with such modifications of the absorption, the interacting light fields undergo a significant variation of the phase shift. It is therefore meaningful to simultaneously measure the absorption coefficient and the index of refraction of these media.

A large number of existing spectroscopic methods allowing simultaneous detection of the absorption and the phase shift are available, but the majority of them do not provide high sensitivity. A critical comparison of several different methods and essential requirements is given in Ref. [4]. A three beam heterodyne interferometer that fulfilled such requirements (simultaneous measurement, shot-noise limited sensitivity, no cross-talk between the absorption and the index of refraction channels, simple signal calibrations, no interaction of the reference light with the sample) was used in our experiment.

With our interferometer we studied the absorption and the index of refraction of either a coupling laser resonant on a hyperfine transition in the caesium D_2 line or a probe laser, while the frequency of the probe laser was scanned over the hyperfine splitting. Different signal profiles were measured: absorption signals, dark resonances or dispersion like profiles; these are discussed and explained.

2. System

The experiment we presented here used a fixed frequency coupling laser, a tunable probe laser and an off-resonant reference laser to measure with a heterodyne technique the probe and the coupling absorption and phase shift in the caesium D_2 line

* Corresponding author. Tel.: +49 511 762 5843; fax: +49 511 762 2784.
E-mail addresses: Luca.Spani.Molella@aei.mpg.de (L. Spani Molella), Rolf-Hermann.Rinkleff@aei.mpg.de (R.-H. Rinkleff).

1386-1425/$ – see front matter © 2005 Elsevier B.V. All rights reserved.
doi:10.1016/j.saa.2005.10.052

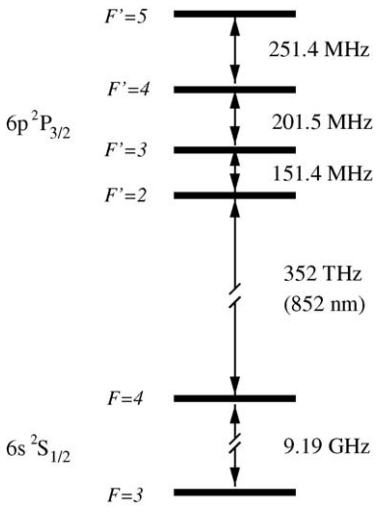

Fig. 1. Energy levels in the Cs D_2 line.

($\lambda = 852$ nm). The caesium energy levels involved in the experiment are shown in Fig. 1. In the configuration discussed in this experiment the ground state hyperfine level $6s\,^2S_{1/2}F = 3$ was coupled by the coupling laser with the excited hyperfine level $6p\,^2P_{3/2}F' = 4$ and the frequency of the probe laser was swept between the hyperfine transition $6s\,^2S_{1/2}F = 4 \rightarrow 6p\,^2P_{3/2}F' = 3$ and $6s\,^2S_{1/2}F = 4 \rightarrow 6p\,^2P_{3/2}F' = 5$.

3. Set-up

A schematic diagram of the experimental set-up is shown in Fig. 2. Since the experimental arrangement resembled another one used in a previous experiment [5], only a general outline will be given here.

3.1. Vacuum system and atomic beam

The experiments were performed in a caesium atomic beam to reduce the influence of Doppler line broadening. A continuous reflux oven [6] produced a beam of caesium atoms with a collimation ratio of 1:50. The atomic beam density in the interaction region was about 4×10^{15} m^{-3} and its width amounted 5 mm. To avoid any collision-generated transfer of population between the Zeeman levels and the caesium gas background, the atomic beam propagated in an ultrahigh vacuum chamber (1 μPa). Six coils in the three spatial directions were mounted outside the vacuum chamber around the interaction region to shield the terrestrial magnetic field below 0.2 μT.

3.2. Laser system and heterodyne interferometer

To simultaneously measure the absorption of an optical transition and the intensity dependent refraction, we used a phase sensitive heterodyne technique [7]. This robust method is orders of magnitude less sensitive to acoustic noise or vibrations than the homodyne interferometer but retains a comparable signal strength. The heterodyne interferometer was constructed with three lasers: coupling, probe and reference. All lasers were single mode diode lasers with an external cavity optical feedback [8,9], i.e., with a resonant optical feedback from a separate optical cavity. Because the frequency noise of such lasers at large Fourier frequencies is strongly reduced in comparison with that of more common diode laser feedback methods constructed with an optical feedback from a grating (such as the Littman set-up and the Littrow set-up) [10], these lasers are well suited for applications where two independent lasers have to be phase locked by means of an optical phase-locked loop. The coupling laser drove the hyperfine transition $6s\,^2S_{1/2}F = 3 \rightarrow 6p\,^2P_{3/2}F' = 4$ and was

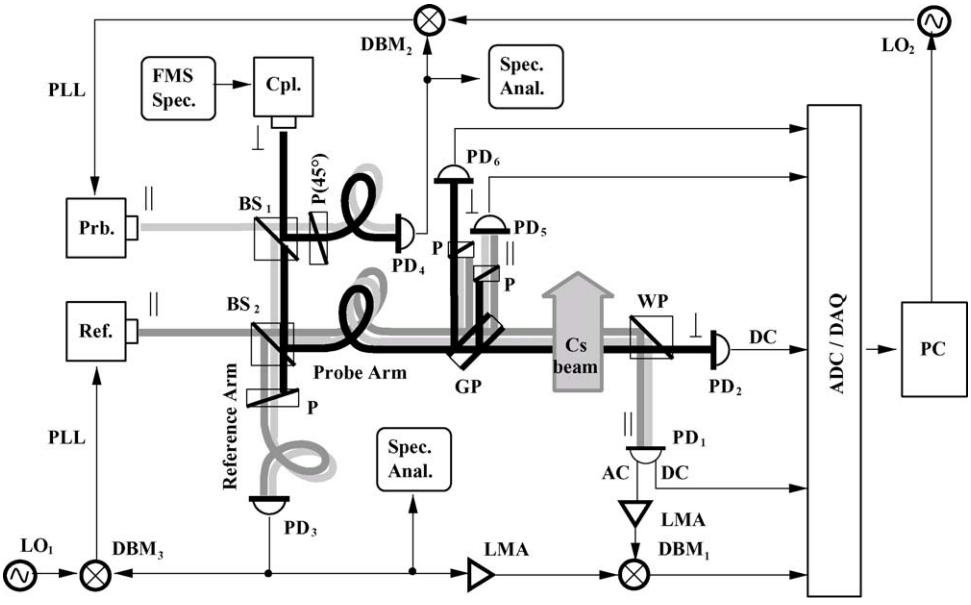

Fig. 2. Experimental set-up for the observation of the transmitted intensities of the coupling and the probe laser and of the phase shift. BS, power beam splitter; DBM, double balanced mixer; GP, glass plate; LMA, limited amplifier; LO, local oscillator; P, polariser; PD, photo-detector; ADC, analog–digital converter; DAQ, data acquisition; PLL, phase-locked loop; Cpl., Ref., Prb., coupling, reference and probe laser.

actively locked to it. The servo loop utilised for this procedure was based on a Doppler-free frequency modulation spectroscopy set-up applied to a caesium cell. As shown in Fig. 2, a further fraction of the coupling power was used as an optical oscillator for phase-locking the probe laser. Applying a tunable ultra stable microwave signal generator (LO_2) and a mixer (DBM_2) the probe laser was detuned with respect to the coupling laser of a frequency difference $d\nu_{pr} \approx \delta + 9.192621$ GHz corresponding to the hyperfine splitting of the caesium ground state added to a detuning δ. Since the beat signal line width measurement was limited by the spectrum analyser resolution bandwidth (3 Hz; sweep time 130 s), we can only give this value as an upper limit for the line width of the frequency difference. The reference laser was phase locked to the probe laser with a constant frequency difference of $d\nu_{ref} \approx 1$ GHz generated by a second microwave signal generator (LO_1), thus not influencing the atomic sample.

The three laser fields were linear polarised: the coupling and the probe field were orthogonally polarised to each other when they entered the vacuum chamber; the polarisation of the reference laser was parallel to that of the probe laser. The laser fields were superimposed at a power beam splitter (BS_2). One output gave origin to the probe arm of the heterodyne interferometer. The light from this output was focused into a single mode fibre, to achieve a good overlap of the modes of the fields. Once superimposed, the three mode-cleaned beams crossed the caesium atomic beam in the interaction zone having a diameter of about 2.2 mm. After the interaction zone the coupling field was separated from the other fields by a Wollaston prism and the intensities were measured by different photo-detectors.

The reference arm of the heterodyne interferometer was located between the second output of the beam splitter (BS_2) and the photodiode used to measure the beat signal between the probe and the reference laser (PD_3). Such a set-up enabled us to measure simultaneously and separately the transmitted intensities of the coupling and the probe field and also the phase shift of the probe field. A similar set-up, following the same inspiring principle but used to measure the phase shift of the coupling laser, is described in detail in Refs. [5,11].

To increase the signal-to-noise ratio of the transmitted intensities we separated a small component of the input laser light by means of a glass plate (GP) situated just before the vacuum chamber (see Fig. 2). With two polarisers we decomposed the polarisation of this derived beam and were therefore able to separately measure a signal proportional to the coupling laser intensity (at the photodiode PD_6) and another one (at the photodiode PD_5) proportional to the sum of the probe and the reference laser intensities immediately before the interaction area. Due to this proportionality, the signals carried information regarding the noise accumulated in the interferometer by the two polarisation channels. Keeping the optical paths for the transmitted intensities as short as possible after the interaction area, and dividing the signals generated by the transmitted intensities with the signals generated by the derived beams with the corresponding polarisation (i.e., filtering out the common noise), one could drastically improve the signal-to-noise ratio, expecially at low transmitted intensities. An example of such an improvement is commented in Section 3.4. To regain the information about the absolute values of the absorptions signals, one can multiply again the results obtained though the division with the average values of the denominators, and, when the reference laser is present, subtract its average contributions to the overall power.

To measure the phase shift of the coupling laser, the polarisation of the coupling laser could be changed to be parallel to that of the reference laser; similarly, the probe polarisation was changed to keep it orthogonal to that of the coupling laser. Furthermore, instead of locking the reference laser and the probe laser, the reference laser was phase locked to the coupling laser with a frequency offset of 1 GHz. This allowed us to simultaneously measure the transmitted intensities of the coupling and probe laser fields and the parametric phase shift of the coupling laser as a function of the probe laser detuning.

3.3. Data acquisition

To record a spectrum, the probe laser frequency was scanned over a 100 MHz frequency interval using a microwave signal generator (Rhode&Schwarz, SMP02). Each measurement acquired about 10,000 points and lasted approximately 2 min. The transmitted intensities of the laser fields were obtained from the DC signals of the photo-detectors PD_1 and PD_2, and the noise of the laser fields from the DC signals of the reference photo-detectors PD_5 and PD_6, respectively.

While the phases and amplitudes in the reference arm were held constant, the phase of the probe field in the probe arm was shifted by $d\phi_{pr}(\delta)$ as a function of the probe detuning δ. As one can see in Fig. 2 the beat signals of the probe and reference arm of the heterodyne interferometer were electronically multiplied by the mixer (DBM_1). The mixer output signal provided then the desired phase information.

The experiment was controlled by a PC running an operating program written in LabVIEW™. Timing, data transfer and microwave signal generators were handled by a National Instruments DAQ card and a GPIB card mounted in the PC. The intensities at the photo-detectors PD_1, PD_2, PD_5 and PD_6 (including the phase signals) were digitised for further digital processing and stored on the computer.

3.4. Noise suppression

As already discussed, the signals recorded at PD_1 and PD_5 carried information on one polarisation of the laser beams and the signals recorded at PD_2 and PD_6 carried information on the orthogonal polarisation. For this reason, dividing the two corresponding signals, i.e., calculating the ratios I_1/I_5 and I_2/I_6 (where I_i represents the intensity at the ith photodiode), one could eliminate the common noise accumulated along the interferometer paths. An example of the improvement obtainable with such a procedure is given in Fig. 3, where the original and the noise-filtered data of a single simultaneous measurement of the coupling and the probe absorption are shown. For completeness we also show the simultaneously taken dispersion measurement of the coupling laser parametric dispersion.

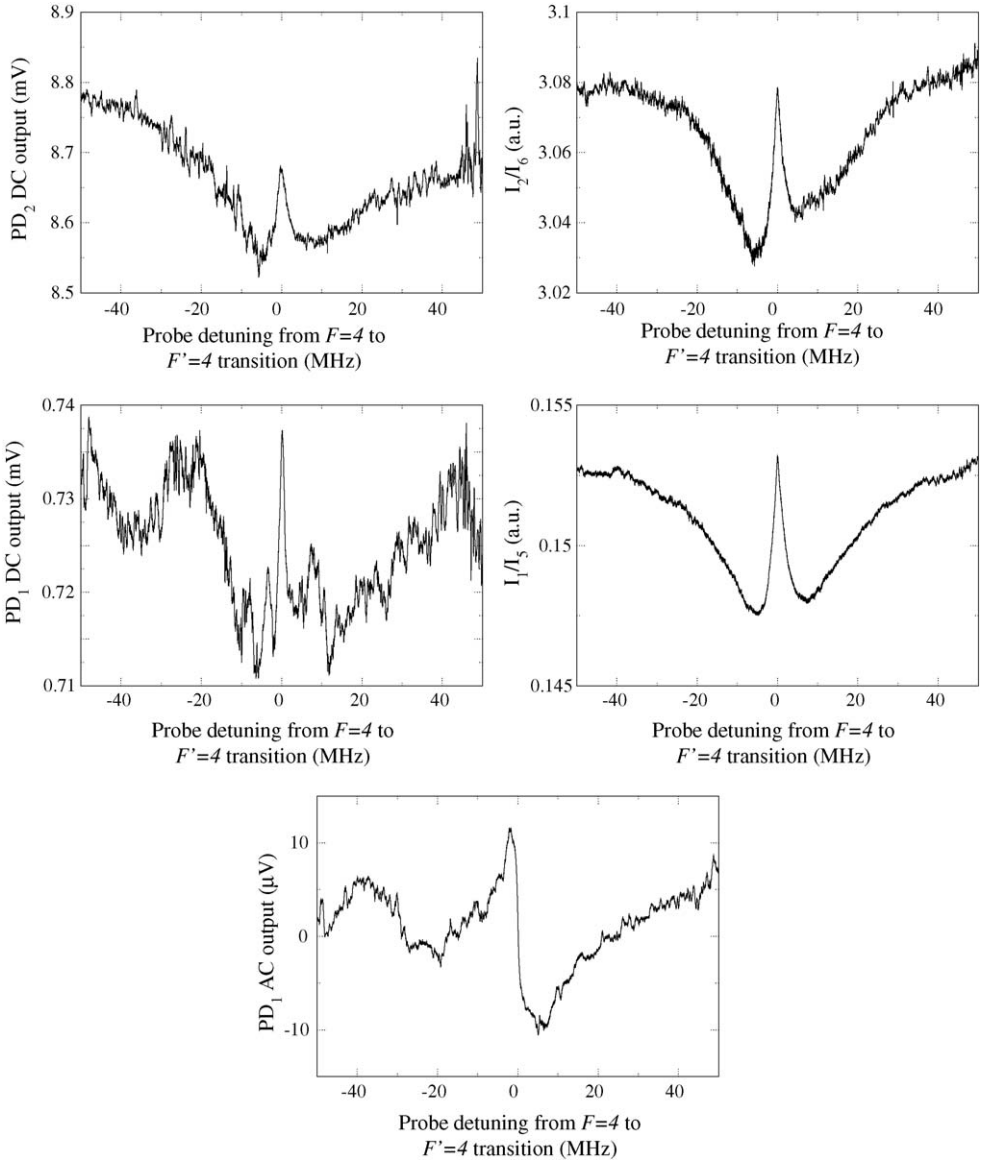

Fig. 3. Simultaneously measured DC transmission signals at PD_1 (centre left) and PD_2 (top left), corresponding noise-filtered signals (centre and top right) and AC signal at PD_1 (corresponding to the phase shift of the coupling laser). Further details in the text.

4. Experiments and results

In all experiments discussed in the following sections, the coupling laser drives the hyperfine transition $6s\,^2S_{1/2}F = 3 \rightarrow 6p\,^2P_{3/2}F' = 4$.

4.1. Absorption

To measure the hyperfine splitting of the level $6p\,^2P_{3/2}$, one needs a frequency tuning range of about 550 MHz. Since our laser system allows only stable tuning ranges of about 100 MHz, we have measured the splitting by overlapping ten 100 MHz scans, each of which was detuned from the previous one by 50 MHz to ensure a good overlap. During these measurements we kept the reference laser off thus not performing any dispersion measurements. Fig. 4 shows the transmitted intensities of PD_1 and PD_2. The excited transitions involved are sketched above the respective absorption measurements. Strong differences between the two spectra were found. With PD_1 we observed two absorption profiles and an absorption signal with a narrow feature at the line centre; with PD_2 an absorption profile, an absorption signal with a narrow feature at line centre and a signal resembling a dispersion profile.

PD_1 recorded the transmitted intensity of the probe laser. When the probe laser frequency was resonant with the hyperfine transition $6s\,^2S_{1/2}F = 3 \rightarrow 6p\,^2P_{3/2}F' = 3$ or $F' = 5$ we measured a usual absorption profile. This is the behaviour that one could expect since, generally, laser light passing through an atomic sample will be strongly absorbed if the laser frequency nears a transition frequency of the atoms.

PD_2 collected the transmitted intensity of the light which was orthogonally polarised with respect to the polarisation of

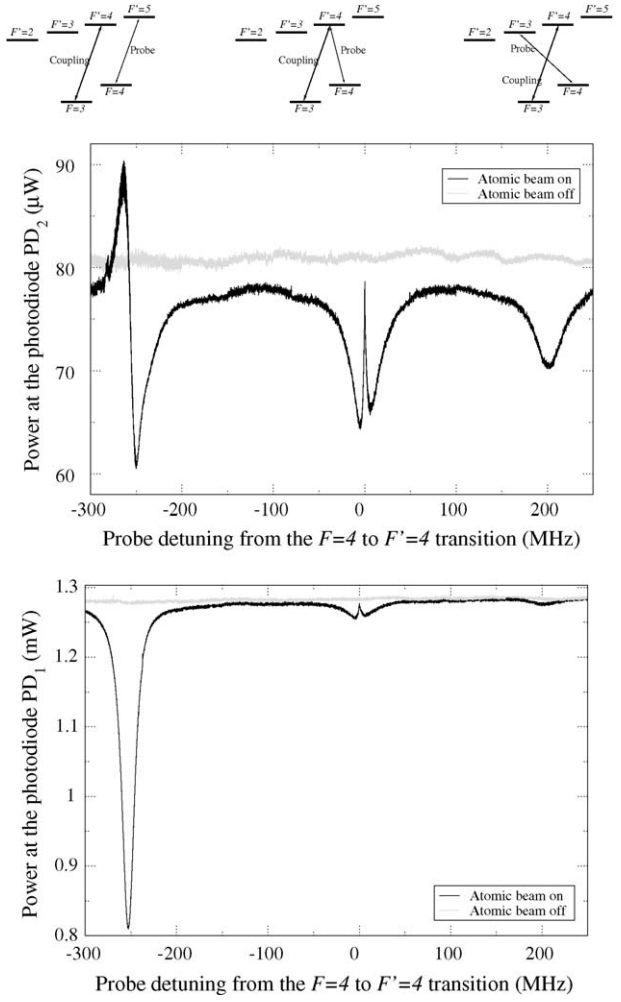

Fig. 4. Transmitted powers observed at PD_1 and PD_2 as a function of the probe laser detuning. PD_1 detected the probe laser intensity and PD_2 the light orthogonally polarised to the probe laser polarisation. Above each resonance the figure shows the corresponding hyperfine transition. Further details in the text.

the probe laser as, for example, the intensity of the coupling laser. The amount of transmitted intensity changed depending on the probe detuning: when resonant, the probe laser induced transitions which modified the former constant absorption level of the resonant coupling laser (this absorption is indeed responsible for the off-resonant gap between the measured values with and without atomic beam). A look at the level diagram (Fig. 4) explains why an absorption profile was detected at PD_2 on the right hand side of the spectrum. The coupling laser depopulated the $6s\,^2S_{1/2}F = 3$ hyperfine level and, as a result of the optical hyperfine pumping, the population in the $6s\,^2S_{1/2}F = 4$ level increased. When the probe laser was in the vicinity of the transition to the excited hyperfine level $6p\,^2P_{3/2}F' = 3$ a re-pumping from the $6s\,^2S_{1/2}F = 4$ level was present and the population in the $6s\,^2S_{1/2}F = 3$ level increased; this led to an increase in the coupling laser field absorption and to the absorption profile detected with PD_2.

4.2. Electromagnetically induced transparency

When the probe laser frequency was scanned around the hyperfine transition $6s\,^2S_{1/2}F = 4 \rightarrow 6p\,^2P_{3/2}F' = 4$ a signal with a dip in the centre was recorded either at PD_1 and at PD_2. In this case the coupling and the probe laser transitions formed a three-level lambda system (Fig. 4). Because of the atomic coherence the transmitted intensities of the coupling and the probe laser exhibited narrow features at the line centre with a half-width-at-half-maximum of about 40 kHz. The opaque medium became nearly completely transparent for both laser fields in the vicinity of the two-photon resonance. This effect, known as electromagnetically induced transparency (EIT), was measured with either photo-detectors, i.e., for the probe and the coupling fields, as expected. A review of this effect is given by Arimondo [2]. Other more recent reviews on specific aspects of EIT and its application can be found in Refs. [12,13].

With a further reference laser, the heterodyne interferometer allowed the simultaneous measurement of the EIT signals and a further phase shift measurement. A typical simultaneous measurement of the probe transmitted intensity (normalised as described in Section 3.4) and of the relative phase shift is shown in Fig. 5. Simultaneously with vanishing absorption, both fields undergo a very rapidly varying phase shift. The probe field dispersion spectrum consists of a normal refractive index profile and a very narrow inverted structure at the two photon resonance (which can be seen in Fig. 5). The phase shift induced in

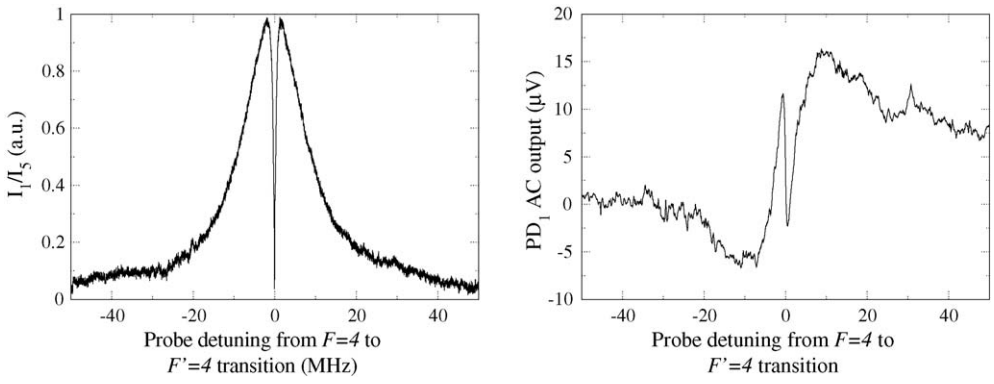

Fig. 5. Typical EIT and relative phase shift signal for the probe laser observed in the Cs system $6s\,^2S_{1/2}F = 3 \rightarrow 6p\,^2P_{3/2}F' = 4$.

the coupling laser field by the tunable probe laser shows only the central structure resulting from the two photon resonance (see Fig. 3). We have called it parametric dispersion. A detailed discussion of this effect is given in Ref. [11].

4.3. Light induced birefringence

In this experiment we had a fully resolved hyperfine structure in the ground and in the excited states. We could neglect the effects of collisions in the ground as well in the excited states (see Section 3.1: atomic beam in high vacuum) and the laser intensity was sufficiently low, to ignore the stimulated emission.

From the level diagram (Fig. 4, top left corner) it could be argued that no influence of the probe laser field was present on the coupling laser field when the probe laser field was resonant with the transition to the hyperfine level $6p\,^2P_{3/2}F' = 5$, because no electric dipole transition was possible from this excited level to the ground level $6s\,^2S_{1/2}\,F = 3$. In addition, no dispersion signal could be detected when we tried to measure the AC contribution of the light orthogonally polarised to that of the probe laser (i.e., the light which, in the case of EIT, gave origin to the so-called parametric dispersion).

The linearly polarised coupling and probe fields had orthogonal polarisation. The coupling field differently populated the Zeeman levels of the excited $6p\,^2P_{3/2}F' = 4$ hyperfine level, in accordance with the transition probabilities. The population of these levels decayed at a rate corresponding to their branching ratios and created an alignment in the $6s\,^2S_{1/2}F = 4$ level [14], which made the atomic sample anisotropic; hence, the absorptions coefficients and the refractive indeces for the left and right circularly polarised light became different. This difference in the refractive index resulted in optical birefringence while the anisotropy in the absorption made the polarisation of the probe beam elliptical.

Let us now consider the polarisation of the probe laser. After the interaction with the atomic sample the linear polarised light of the probe laser crossed a Wollaston prism and was consequently decomposed into two linear polarisations perpendicular to each other. On account of the optical sample birefringence the polarisation axis rotated and extra intensity coming from the probe laser was detected on photo-receiver PD_2. The linear polarisation of the probe could be decomposed into a left and a right circular polarisation with the same transition frequency. Since the frequency dependence of the refractive index was dispersive for each polarisation, the difference led to a dispersive signal. The contribution of the intensity of the probe light on PD_2 is here given up to second-order from Ref. [15] as:

$$I(\Phi) = \left\{ \sin^2\Phi + \Delta\theta \sin 2\Phi + \left[(\Delta\theta)^2 + \left(\frac{\Delta\alpha L}{4} \right)^2 \right] \cos^2\Phi \right\} I_{\mathrm{pr}} \exp(-\alpha L),$$

where Φ is the small angle deviation from the axis perpendicular to the polarisation axis of the probe light and $\Delta\theta = (n_+ - n_-)k_0 L/2$ the phase difference between the two circularly polarised components. L is the interaction length of the probe laser with the atomic sample; $\Delta\alpha$ and α represent the difference and the sum of the absorption coefficients for left and right circularly polarised components, respectively.

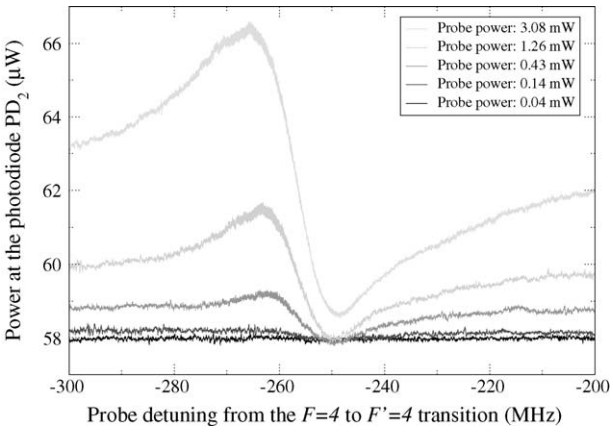

Fig. 6. Transmitted power detected at PD_2. Light induced birefringence as a function of the probe laser power.

If the axis of the analyser had been exactly perpendicular to the direction of the polarisation ($\Phi = 0$) then no dispersion shape could have been measured. A small deviation from the perpendicular adjustment was needed, so that the term $\Delta\theta \sin 2\Phi$ gave the main contribution to the signal, while $\sin^2\Phi$ contributed to the signal only with an offset.

As a an additional proof we also measured the dependence of the laser light induced birefringence on the intensity of both lasers. We observed no significant dependence of the dispersion-like absorption profile measured with PD_2 on the coupling laser intensity when the probe laser power was kept constant. Conversely, as shown in Fig. 6, the light induced birefringence amplitude showed a strong variation as a function of the probe laser power (keeping the coupling laser power constant). This demonstrated its origin as a probe laser generated effect and confirmed the explanation given above.

5. Conclusion

We have studied over a frequency range of about 550 MHz the transmitted intensities of a coupling and a probe lasers interacting with a caesium atomic beam with a heterodyne interferometer which allowed simultaneous measurements of absorption and phase shift. We have presented a technique to improve the signal-to-noise ratio of such an interferometer by using an auxiliary optical path. With such a setup different signals could be measured (absorption profiles, EIT signals and a dispersion-like absorption profile) and their origin was subsequently explained. In particular we have confirmed the dependence of laser light induced birefringence on the probe laser power, demonstrating its appearance in a collinear experimental set-up.

Acknowledgement

This project was supported by the Grant No. SFB407 of the Deutsche Forschungsgemeinschaft.

References

[1] L. Allen, J.H. Eberly, Optical Resonance and Two-Level Atom, John Wiley & Sons, New York, 1975.
[2] E. Arimondo, in: E. Wolf (Ed.), Progress in Optics, vol. 35, Elsevier Science, Amsterdam, 1996, pp. 257–354.
[3] A.M. Akulshin, S. Barreiro, A. Lezama, Phys. Rev. Lett. 83 (1999) 4277.
[4] A. Wicht, M. Müller, V. Quetschke, R.-H. Rinkleff, A. Rocco, K. Danzmann, Appl. Phys. B 70 (2000) 821.
[5] M. Müller, F. Homann, R.-H. Rinkleff, A. Wicht, K. Danzmann, Phys. Rev. A 62 (2000) 060501(R).
[6] R.D. Swenumson, U. Even, Rev. Sci. Instrum. 52 (1981) 559.
[7] G. Müller, A. Wicht, R.-H. Rinkleff, K. Danzmann, Opt. Commun. 127 (1996) 37.
[8] B. Dahmani, L. Hollberg, R. Drullinger, Opt. Lett. 12 (1987) 876.
[9] R.W. Fox, C.W. Oates, L. Hollberg, in: R. van Zee, J. Looney (Eds.), Cavity Enhanced Spectroscopy, vol. 40, Academic Press, Amsterdam, 2002, pp. 1–46.
[10] C. Wieman, L. Hollberg, Rev. Sci. Instrum. 62 (1991) 1.
[11] M. Müller, F. Homann, R.-H. Rinkleff, A. Wicht, K. Danzmann, Phys. Rev. A 64 (2001) 013803.
[12] M.D. Lukin, P. Hemmer, M.O. Scully, in: B. Bederson, H. Walther (Eds.), Advances in Atomic, Molecular, and Optical Physics, vol. 42, Academic Press, New York, 2000, pp. 347–384.
[13] N.V. Vitanov, M. Fleischhauer, B.W. Shore, K. Bergmann, in: H. Walther, B. Bederson (Eds.), Advances in Atomic, Molecular, and Optical Physics, vol. 46, Academic Press, New York, 2001, pp. 55–180.
[14] A. Omont, Prog. Quantum Electron. 5 (1977) 69.
[15] Y. Yoshikawa, T. Umeki, T. Mukae, Y. Torii, T. Kuga, Appl. Opt. 42 (2003) 6645.